Methane on the Rise—Again

Euan G. Nisbet *et al.*

Science **343**, 493 (2014);
DOI: 10.1126/science.1247828

Science (print ISSN 0036-8075; online ISSN 1095-9203) is published weekly, except the last week in December, by the American Association for the Advancement of Science, 1200 New York Avenue NW, Washington, DC 20005.

tron and hole at room temperature and generation of free charge carriers.

The large exciton binding energies in π-conjugated materials are related not only to their low dielectric constants (which offer less screening between charges and lead to stronger interactions) but also to the presence of strong electron-vibration and electron-electron interactions (*5*). Because excitons are neutral species unable to carry a current, the efficiency of organic solar cells depends critically on charge-separation processes at heterojunctions between an electron donor (D; typically a π-conjugated polymer or molecule) and acceptor (A; typically a fullerene derivative), such as those displayed in the figure. These D-A heterojunctions are required to produce a driving force to dissociate excitons into spatially separated charges and are generally considered as an important factor limiting efficiency compared to inorganic p-n junction solar cells [the efficiency of crystalline silicon solar cells is on the order of 25% (*2*)]. Understanding the energy-harvesting mechanisms in organic solar cells, thus requires the ability to characterize the elementary charge-generating processes as a function of materials choice and in the presence of multiple nano- and mesoscale morphological variations.

From an electronic-structure standpoint, when an exciton appears at the D-A interface, the exciton state can evolve into a charge-transfer (CT) state and eventually into a charge-separated state (*5*). A CT state is a D-A interfacial state for which a hole on a donor molecule or polymer segment is located next to an electron on an acceptor (fullerene) molecule. In the CT state, the electron and hole are still electrostatically bound to one another; as a result, there is limited electronic polarization of the surrounding molecules because the CT exciton is neutral. For the electron and hole to separate, they have to overcome their Coulomb attraction; this is facilitated by an increased electronic polarization of the surrounding molecules, which stabilizes the separated charges.

Gélinas *et al*. developed ultrafast spectroscopic tools that resolve the electron-hole separation in the femtosecond regime. They exploit the signature of the electric field that is generated between the electron and the hole as they separate. This field alters the molecular orbital energies of the surrounding molecules and thus their optical transition energies, i.e., it leads to an electro-absorption (EA) signal (*6*). Gélinas *et al*. could measure the EA signals with <30-fs precision and quantify the electrostatic energy stored in the electric field. In this way, they could characterize the initial steps of electron-hole separation as they occur in the tens of femtoseconds regime (*4*). The authors measured two model systems, consisting of a small molecule–fullerene blend (illustrated in the figure) and a polymer-fullerene blend, and varied the D-A compositions. In the blends with compositions leading to high power conversion efficiencies, there appears a clear EA signal indicative of long-range separation of electrons and holes. For the polymer-fullerene blend, the electrostatic energy between electron and hole reaches up to ~0.2 eV (about eight times the thermal energy at room temperature) within 40 fs of excitation, at which time the electron has left the hole some 4 to 5 nm behind and the charges can move apart freely. Efficient separation is accomplished without requiring excess energy beyond that needed to overcome Coulomb attraction, which is in line with recent results from Vandewal *et al*. (*7*).

Although providing a much needed characterization of the charge-separation process as it occurs at D-A interfaces, the work of Gélinas *et al*. opens up many intriguing questions, particularly with regard to the nature of the interfacial morphology and electronic structure that enables ultrafast charge separation. The authors suggest that relatively ordered domains of fullerenes at the D-A interface allow the electrons to access delocalized "bandlike" states. It remains to be seen what happens in the regions where donors and acceptors are mixed and disordered, which are often invoked as a key component of efficient solar cells (*8*). Also, most of the energetic analyses to date have focused on enthalpy considerations. Reaching a complete picture will require including the role of entropy (*9*), in addition to obtaining an accurate description of the polarization effects.

References

1. C. W. Tang, *Appl. Phys. Lett.* **48**, 183 (1986).
2. See www.nrel.gov/ncpv/images/efficiency_chart.jpg.
3. R. A. J. Janssen, J. Nelson, *Adv. Mater.* **25**, 1847 (2013).
4. S. Gélinas *et al*., *Science* **343**, 512 (2014); 10.1126/science.1246249.
5. J. L. Brédas *et al*., *Acc. Chem. Res.* **42**, 1691 (2009).
6. L. Sebastian *et al*., *Chem. Phys.* **61**, 125 (1981).
7. K. Vandewal *et al*., *Nat. Mater.* **13**, 63 (2014).
8. P. Westacott *et al*. *Energy, Environ. Sci.* **6**, 2756 (2013).
9. B. A. Gregg, *J. Phys. Chem. Lett.* **2**, 3013 (2011).

10.1126/science.1249230

ATMOSPHERIC SCIENCE

Methane on the Rise—Again

Euan G. Nisbet,[1] Edward J. Dlugokencky,[2] Philippe Bousquet[3]

Atmospheric concentrations of the greenhouse gas methane are rising, but the reasons remain incompletely understood.

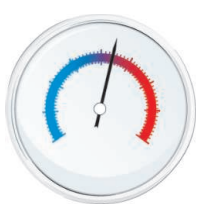

Roughly one-fifth of the increase in radiative forcing by human-linked greenhouse gases since 1750 is due to methane. The past three decades have seen prolonged periods of increasing atmospheric methane, but the growth rate slowed in the 1990s (*1*), and from 1999 to 2006, the methane burden (that is, the total amount of methane in the air) was nearly constant. Yet strong growth resumed in 2007. The reasons for these observed changes remain poorly understood because of limited knowledge of what controls the global methane budget (*2*).

Estimates of methane emissions vary widely. Global estimates derived from process studies of sources (termed "bottom-up") are generally much larger than those from direct observation of the air ("top-down") (*2*). Local industrial emissions may be far underestimated (*3*). The renewed rise in the methane burden prompts urgent questions about the causes, but globally, in situ monitoring to track atmospheric methane is very limited outside the major nations.

Methane sources and sinks vary with latitude. Overall, about two-thirds of the emissions are caused by human activities; the remaining third is from natural sources. At polar latitudes, methane sources include wetlands, natural gas wells and pipelines, thawing permafrost, and methane hydrate associated with decaying offshore permafrost. In

[1]Department of Earth Sciences, Royal Holloway, University of London, Egham TW20 0EX, UK. [2]National Oceanic and Atmospheric Administration, Earth System Research Laboratory, Boulder, CO 80305, USA. [3]Laboratoire des Sciences du Climat et de l'Environnement, CEA-CNRS-UVSQ, Saclay, 91191, Gif-sur-Yvette, France. E-mail: e.nisbet@es.rhul.ac.uk

CREDIT: V. ALTOUNIAN/*SCIENCE*

the heavily populated northern mid-latitudes, the main sources are the gas and coal industries, agriculture, landfills, and biomass fires. Tropical wetlands are the world's largest natural source of methane (*4*). Emissions from equatorial and savanna wetlands, ruminants, and biomass burning are increased further by tropical anthropogenic inputs. The main methane sink is reaction with hydroxide radicals (OH), especially in the tropical mid-troposphere. Minor sinks include soil oxidation, reaction with marine chlorine, and reactions in the stratosphere.

From the 1980s until about 1992, atmospheric methane was rising sharply by about 12 parts per billion (ppb) per year (see the first figure). Then came a decade of much slower growth (by about 3 ppb/year) coupled to a sudden decrease in the north-south interpolar difference (*1*). In the early 2000s, growth almost ceased; for short periods, the total methane burden even declined. For the "stagnation" period from 1999 to 2006, these top-down findings from atmospheric data differ markedly (*5*) from bottom-up inventories, which detail strong growth in anthropogenic emissions. Yet the main sink—oxidation by OH—sees little changed (*4*). This discrepancy between top-down and bottom-up budgets remains unresolved.

In 2007, just when scientists thought the methane concentration had stabilized, it rose again. Since then, global average growth has been ~6 ppb/year. Considering the latitudinal zones in more detail (see the second figure), Arctic methane rose more than the global growth rate in 2007, but since then Arctic growth has tracked global trends. Large emissions attributed to decaying methane hydrates have been reported from the East Siberian Arctic Shelf (*6*) but are not apparent in NOAA atmospheric observations, nor are they detected in isotopic measurements from surface and aircraft sampling in the European Arctic (*7*), which point to wetlands as a major Arctic source in summer and industrial gas leaks in winter. Long-term release of methane from hydrate is probable (*8*), but catastrophic hydrate emission scenarios (*9*, *10*) are unlikely.

In the southern tropics, growth has been above global trends since 2007 (see the second figure). For example, at Ascension Island (8°S), sampling the tropical South Atlantic, growth was >10 ppb per year in 2009 and 2010, when wet regional summers would have led to expanded wetland areas. This was part of a regional 5-year rise in natural emissions that may give insight into past glacial terminations and initiations, when the methane burden changed sharply, perhaps from similar processes.

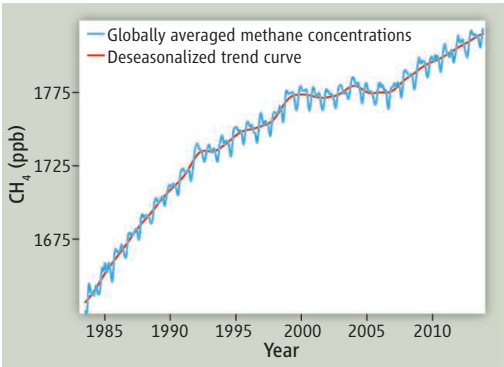

Methane ups and downs. Globally averaged atmospheric methane concentrations rose quickly before 1992. The rise then slowed and almost stopped between 1999 and 2006, but resumed in 2007. Data from ftp://ftp.cmdl.noaa.gov/ccg/ch4/flask/event/.

Atmospheric data show that global emissions were ~15 to 22 Tg (million tons) CH_4 per year greater in 2010 than in 2005. Global-scale modeling of these methane observations (*4*, *5*, *11*) suggests that in 2007, tropical wetland emissions dominated growth, with output from high northern latitudes also important. Since then, the increase has mostly been driven by the tropics (9 to 14 Tg/year) and northern mid-latitudes (6 to 8 Tg/year) (*11*).

There is much to suggest that emissions from human activities have also increased since 2007. In the United States, which has overtaken Russia as the largest gas producer (*12*), hydraulic fracturing is increasingly important. In Utah, fracking may locally leak 6 to 12% of gas production to the air (*13*). A full understanding of the greenhouse impact of fracking requires monitoring over the gas-well lifetime and analysis of the transport distribution system. Global coal mining has also expanded dramatically (*12*), especially in China. Rising energy production suggests increased emission from these human activities, but this inference needs to be reconciled with observations on ^{13}C in methane; since 2007, atmospheric methane has become more depleted in ^{13}C (*14*), an indication that growth is dominated by ^{12}C-richer wetland and ruminant emissions.

More data are needed to resolve the divergence between top-down and bottom-up estimates, but the measurement network for methane concentration and isotopes is very thin. At a meeting of the European Pergamon Arctic methane group in Kiel, Germany, in November 2013, Crill commented that "data without models are chaos, but models without data are fantasy." Spatially and temporally, better measurement is essential to identify and quantify methane sources (*3*, *4*, *12*), but long-term data gathering is in trouble. Despite methane's attractiveness as a cost-effective greenhouse reduction target, budgets for greenhouse gas monitoring are contracting. Somewhere, perhaps in the tropics or East Asia, unwelcome methane surprises may lurk, but watchers are few.

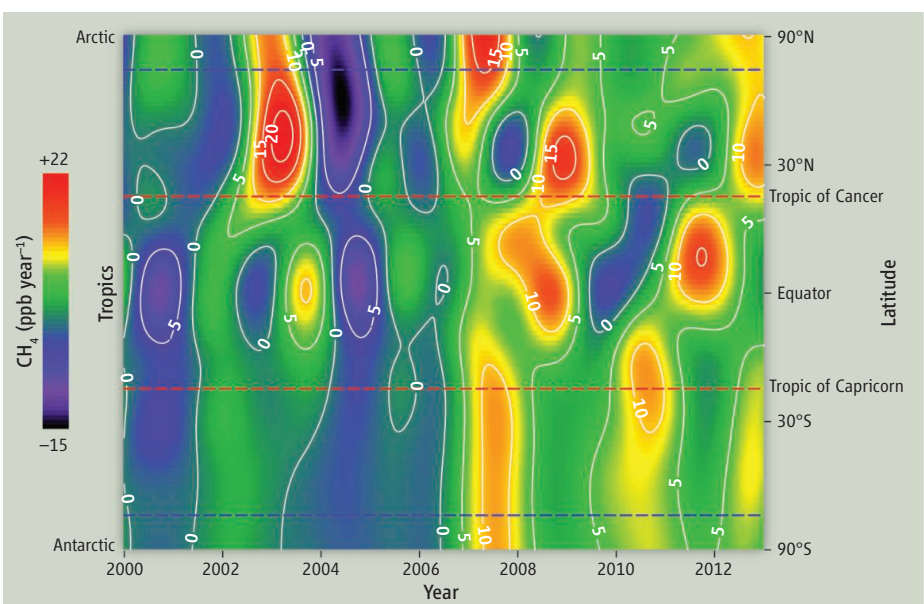

Methane growth rate by latitude. Contours of methane growth rate with sine of latitude. Plotting by sine of degree of latitude equally weights the results for surface area with latitude. Data from www.esrl.noaa.gov/gmd/ccgg/mbl/.

References and Notes

1. E. J. Dlugokencky, E. G. Nisbet, R. Fisher, D. Lowry, *Philos. Trans. R. Soc. London Ser. A* **369**, 2058 (2011).

CREDITS: (A) E. J. DLUGOKENCKY; (B) K. MASARIE, NOAA

Published by AAAS

2. S. Kirschke *et al.*, *Nat. Geosci.* **6**, 813 (2013).
3. S. M. Miller *et al.*, *Proc. Natl. Acad. Sci. U.S.A.* 10.1073/pnas.1314392110 (2013).
4. P. Bousquet *et al. et al.*, *Atmos. Chem. Phys.* **11**, 3689 (2011).
5. I. Pison *et al.*, *Atmos. Chem. Phys.* **13**, 11609 (2013).
6. N. Shakhova *et al.*, *Nat. Geosci.* **7**, 64 (2014).
7. R. E. Fisher *et al.*, *Geophys. Res. Lett.* **38**, L21803 (2011).
8. A. Biastoch *et al.*, *Geophys. Res. Lett.* **38**, L08602 (2011).
9. G. Whiteman *et al.*, *Nature* **499**, 401 (2013).
10. See also http://equianos.com/wordpress/wp-content/uploads/Response-to-Whiteman_et-al-Comment.pdf.
11. P. Bergamaschi *et al.*, *J. Geophys. Res.* **118**, 7350 (2013).
12. BP Statistical Review of World Energy 2013; www.bp.com/statisticalreview.
13. A. Karion *et al.*, *Geophys. Res. Lett.* **40**, 4393 (2013).
14. See ftp://aftp.cmdl.noaa.gov/data/trace_gases/ch4c13/flask/.

Acknowledgments: Supported in part by the UK Natural Environment Research Council MAMM and Tropical Methane projects, the European Union's Ingos project, and Royal Holloway.

10.1126/science.1247828

APPLIED PHYSICS

Selecting the Direction of Sound Transmission

A device containing a circulating fluid breaks the symmetry of acoustic waves and allows one-way transmission of sound.

Steven A. Cummer

Structures that admit flow in only one direction are commonplace—consider one-way streets, insect traps, and the staple of the police procedural story, the one-way mirror. However, creating a device that allows waves to pass in only one direction, termed an isolator, is challenging because of the inherently symmetric physics of wave phenomena. On page 516 of this issue, Fleury *et al*. (*1*), taking inspiration from a natural electromagnetic phenomenon, designed and demonstrated an engineered structure that allows one-way transmission of sound waves.

Creating a one-way, or nonreciprocal, structure for general wave flow is more challenging than one might think. The one-way mirror, for example, is not truly a nonreciprocal optical wave device, as the effect is created primarily by a trick of unequal lighting. True nonreciprocity in linear materials is tied to breaking of time-reversal symmetry (*2*). A system exhibits time-reversal symmetry if one solution of the entire system, but run backward in time, is a second solution. This condition is equivalent to interchanging the source and receiver sides of the problem, as illustrated in panel A of the figure. Wave phenomena by their nature generally exhibit time-reversal symmetry (consider how circular ripples on a pond surface can be either outwardly expanding or inwardly converging), so creating a nonreciprocal device or medium takes something special.

Engineering wave propagation nonreciprocity into materials is an area of substantial recent research. There are several different ways to do this, which are summarized in clear and thorough reviews in the context of acoustic (*3*) and electromagnetic (*4*) waves. Interestingly, many efforts that have demonstrated asymmetric power transmission for specific input and output field distributions are not truly nonreciprocal and cannot be used to create general nonreciprocal devices (*3*, *4*). Carefully designed nonlinear structures can exhibit nonreciprocity without time-reversal asymmetry (*3*, *4*), but this approach results in constraints like amplitude dependence that limit its value in wave isolator applications.

It turns out that linear systems that contain a directional bias that is defined by some form of internal motion (a so-called odd vector under time reversal) can be made nonreciprocal (*2*). In such a system, strict time reversal reverses the direction of that internal motion and reverses the bias direction as well. Such systems would be reciprocal if the internal motion, and thus the directional bias, is also reversed when the input and outputs are swapped, in accord with time reversal. Interchanging the input and output ports without reversing the direction of the bias creates a nonreciprocal device by breaking time-reversal symmetry, as illustrated in panel B of the figure.

Some materials naturally contain this kind of directional bias and are inherently nonreciprocal—for example, the ionized gas of Earth's upper atmosphere permeated by the directional bias of the steady geomagnetic field (*5*). An external magnetic field can also be applied to magnetically active materials, such as ferrites to create nonreciprocity. This approach is used in many practical nonreciprocal optical or radio-frequency isolators (*6*).

In contrast, linear acoustic nonreciprocity had not, until now, been demonstrated except in weak or large-scale forms not suitable for compact applications. Fleury *et al*. have now done precisely that by borrowing the basic physics of the Zeeman effect, in which a biasing magnetic field creates a strongly birefringent medium in which different polarization states interact with different medium resonances. Because this is an effect created by a fixed bias field, such a medium is nonreciprocal. Fleury *et al*. (*1*) create analogous acoustic resonance splitting in a compact circular cell that contains a rotational mean air flow. Counterpropagating acoustic waves in this cell experience different resonant frequencies, an effect that can be derived both from the basics of acoustic wave propagation in a steady mean flow and from a quantum-mechanical operator approach [see the supplementary materials of (*1*)].

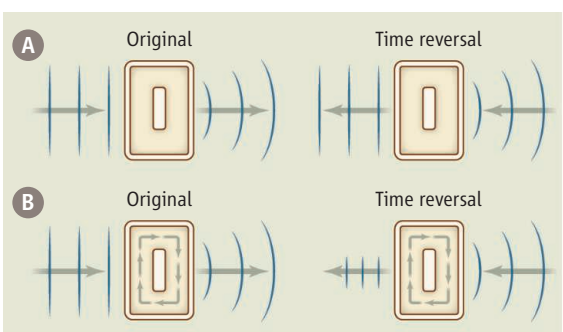

Obeying and breaking time-reversal symmetry. (A) In a material or device without a preferred direction, the fundamentally symmetric behavior of waves means that a solution runs backward in time and is still a solution. This condition is equivalent to interchanging the input and output waves in the system. **(B)** However, if the system contains a flow-based directional bias, and that bias is not flipped when the input and output waves are interchanged, then time-reversal symmetry is broken. Wave transmission through such a system can be dramatically different when the input and outputs are interchanged, and thus nonreciprocal.

Department of Electrical and Computer Engineering, Duke University, Durham, NC 27708, USA. E-mail: cummer@duke.edu